This article has been accepted for publication in a future issue of this journal, but has not been fully edited. Content may change prior to final publication. Citation information: DOI 10.1109/TMC.2020.3000503, IEEE Transactions on Mobile Computing

Hybrid OFDMA Random Access with Resource Unit Sensing for Next-gen 802.11ax WLANs

Leonardo Lanante Jr, *Member, IEEE* Chittabrata Ghosh, *Senior Member, IEEE* and Sumit Roy, *Fellow, IEEE*

Abstract—IEEE 802.11ax partitions a regular 20MHz channel into smaller sub-channels called resource units to support simultaneous multiuser operation using Orthogonal Frequency Division Multiple Access (OFDMA). Uplink OFDMA Random Access (UORA) in IEEE 802.11ax allows stations to transmit via a scheduled random access mechanism. UORA is initiated via a trigger frame which aside from serving as a synchronization mechanism, also informs stations which resource units are allowed for random access. Using the trigger frame information, the stations engage in an OFDMA backoff process to win access to a resource unit. Similar to slotted ALOHA, the maximum normalized throughput of UORA is only 37% due to high probability of collisions at high loads. To reduce collisions, we equip UORA with carrier sensing capability resulting in a *new* uplink hybrid UORA (H-UORA) OFDMA access mechanism. Unlike other multi-carrier CSMA methods previously proposed in literature, H-UORA is an easily implementable modification to current 802.11ax WLANs. We show that H-UORA can achieve a normalized throughput of at least 80% (which increases further depending on the buffering capabilities of the access point) using various numerical analysis and simulations.

Index Terms—Access schemes, Algorithm/protocol design and analysis, Standards, Wireless systems.

1 Introduction

Uplink (UL) multiuser (MU) transmission using orthogonal frequency division multiple access (OFDMA) is one of the key new innovations in the soon to be concluded High Efficiency (HE) WLAN IEEE 802.11ax amendment [1]. UL OFDMA benefits are three-fold: (i) increased spectral efficiency due to multiple user allocations over a 20 MHz channel bandwidth, (ii) amortization of the preamble with multiple simultaneous transmissions, and (iii) range extension due to frame transmission with increased power spectral density over sub-multiple of 20MHz channel bandwidth. Through the use of narrower resource unit (RU) allocations, multiple stations (STA) can send packets simultaneously, eliminating the overhead from individual channel contentions and block acknowledgments (BA). For a tutorial introduction to UL OFDMA and other advanced 802.11ax features, see [2] and [3].

To enable UL MU transmissions, 802.11ax defines a new control frame called the trigger frame (TF). TF serves as a synchronization mechanism for UL MU access (a timing reference to ensure UL STAs transmit simultaneously) as well as a way to notify the STAs their respective resource unit (RU) allocations (contained in the TF payload) designated by the access point (AP) scheduler. Upon receiving the TF, the targeted STAs send their UL data simultaneously in their allotted RUs using a PHY protocol data unit (PPDU) frame format called the HE Trigger Based (TB) PPDU. When the buffer status of all STAs are known to the AP, UL MU transmission performance can have significant gains over the legacy carrier sense multiple access (CSMA) scheme.

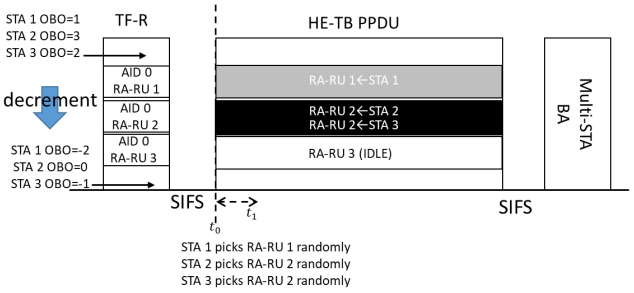

Fig. 1. 802.11ax UL OFDMA-based random access procedure.

Since there are many cases when a STA's buffer access is *unknown* (e.g. STAs that have just woken up from power save mode or unassociated STAs), 802.11ax allows STAs with *unknown buffer status* to participate in UL transmission via OFDMA random access (UORA) mechanism. Here, the AP allocates random access RUs (RA-RUs) that can be used by STAs that do not have RUs dedicated to them. A TF with at least one RA-RU is called the TF-R to denote the fact they trigger random access UL transmissions. STAs identify the RA-RUs in the TF via an association ID (AID) that takes values of either 0 or 2045. Associated STAs only use RA-RUs with AID of 0 whereas un-associated STAs use RA-RUs with AID of 2045.

As stated, the main advantage of UORA is that it does not require STA buffer status information. In addition, it uses a low complexity backoff mechanism called the OFDMA backoff (OBO) to reduce the number of collisions.

- *L. Lanante, is with the Graduate School of Computer Systems and Systems Engineering, Kyushu Institute of Technology, Iizuka, Fukuoka Japan, 820-0053 (leonardo@cse.kyutech.ac.jp)*
- *S. Roy is with Dept. of Electrical & Comp. Engineering, University of Washington, Seattle, WA 98195; (sroy@uw.edu)*
- *C. Ghosh is with Intel Corporation, 2200 Mission College Blvd., Santa Clara, CA 95054; (chittabrata.ghosh@intel.com)*

However, even with optimal OBO parameters, the UORA maximum normalized throughput is only 37% which is low compared to scheduled UL MU access or legacy CSMA [4].[1] This low throughput is directly attributable to the limitation of the OBO mechanism shown in Fig. 1. In UORA, the OBO mechanism works as follows: STAs generate (independently) a random OBO count which they decrement by the number of RA-RUs present in any received TF-R. When the OBO decrements to 0 or a negative value, the STA is granted a transmit opportunity (TXOP) to transmit on a single RA-RU (randomly chosen from among the RA-RU block) on the immediately following UL MU transmission. Since transmitting STAs do not know the chosen RA-RUs of other transmitting STAs, collisions are unavoidable (e.g. STA 2 and STA 3 in the figure).

In this paper, we propose a *new hybrid UORA (H-UORA)* method which combines the OBO mechanism with (fine grained) carrier sensing over RUs to further reduce collisions.[2] H-UORA reduces the probability of collision by allowing transmissions in multiple time slots within the HE-TB PPDU. In Fig. 1 for example, STA 3 could delay transmission from t_0 to a later time t_1 within the HE-TB PPDU duration. From t_0 to t_1, it performs RU sensing (RS) to discover which RA-RUs are idle and which are busy. After discovering that only RA-RU 3 is idle, it transmits in RA-RU3 at t_1. The main drawback of H-UORA is that while the required sub-20MHz channel sensing (i.e. RU sensing) has been proposed in the literature [6], [7], it is yet to be supported in 802.11ax (and in effect, our work makes a case for this).

The contributions of this paper are the following:

1) We develop an analytical model for multi-carrier CSMA (MC-CSMA) that are constrained to small number of RU sensing slots. Unlike the generalized MC-CSMA analyzed in [7], trigger based MC-CSMA (TB-MC-CSMA) like H-UORA is constrained to a few number of carrier sensing slots to prevent deep buffering requirements in the AP.
2) Guided by 1), we propose H-UORA - a new multi-carrier random access method that achieves a high normalized throughput while retaining all the advantageous properties of the conventional UORA, i.e. backward compatibility with scheduled OFDMA access, and distributed OBO based contention.

The rest of the paper is structured as follows. First, a list of all abbreviations is provided in Table 1. We then undertake a survey of related works in Section 2. In Section 3, we introduce the conventional UORA algorithm and explain its low throughput. In Section 4, we derive an analytical model for TB-MC-CSMA which we use to develop the proposed H-UORA algorithm in Section 5. We verify the performance of H-UORA using various numerical results in 6 and proceed with its optimization in Section 7. In Section 8, we discuss various implementation considerations with RU sensing and power leakages that may affect real world performance of H-UORA. Finally, we conclude the paper in Section 9.

1. The normalized throughput is derived in [5] for a single stream UL OFDMA transmission. Multiple spatial streams UORA is currently not supported in 11ax as of the latest draft [1].

2. Since our main focus is UORA, other 11ax features that has no direct effect on its performance are left out of the scope of this paper (e.g. MU-MIMO, Spatial Reuse, Preamble Puncturing, etc.).

TABLE 1
Terms and Abbreviations

Abbreviation	Full name
ACK	Acknowledgment
AID	Association Identifier
A-MPDU	Aggregated MDPU
AP	Access Point
BA	Block ACK
BSR	Buffer Status Report
BSRP	Buffer Status Report Poll
BSS	Basic Service Set
CS	Carrier Sense
CSMA	Carrier Sense Multiple Access
CSMA/CA	Carrier Sense Multiple Access / Collision Avoidance
DL	Downlink
FFT	Fast Fourier Transform
HE	High Efficiency
HE-LTF	HE Long Training Field
HE-STF	HE Short Training Field
HE-TB PPDU	HE Trigger Based PPDU
H-UORA	Hybrid UORA
LAN	Local Area Network
L-SIG	Legacy Signal Field
MAC	Medium Access Control layer
MC-CSMA	Multicarrier CSMA
MIMO	Multiple Input Multiple Output
MPDU	MAC Protocol Data Unit
MU	Multiuser
MU-MIMO	Multiuser Multiple Input Multiple Output
MU-CTS	Multiuser Clear to Send
MU-RTS	Multiuser Request to Send
OCW	OFDMA Contention Window
OBO	OFDMA Backoff
OFDM	Orthogonal Frequency-Division Multiplexing
OFDMA	Orthogonal Frequency-Division Multiple Access
PHY	Physical Layer
PIFS	PCF InterFrame Space
PPDU	PHY Protocol Data Unit
RA-RU	Random Access RU
RS	RU Sensing
RTS	Request to Send
RU	Resource Unit
SIFS	Short InterFrame Space
STA	Station
TB	Trigger Based
TB-MC-CSMA	Trigger Based Multicarrier CSMA
TF	Trigger Frame
TF-R	Trigger Frame for Random Access
TXOP	Transmit Opportunity
UL	Uplink
UORA	UL OFDMA Random Access
WLAN	Wireless LAN

2 Related Works

UORA concept was first proposed by one of the co-authors [8] for 802.11ax to enable random access in UL MU transmissions. The feature addresses some use cases where scheduled UL MU access is inefficient or impossible (e.g. initial link setup traffic in dense public places) due to the unavailability of STA buffer status information by the AP. UORA was shown to have a maximum normalized throughput equal to 37% similar to slotted ALOHA. More accurately however, UORA is a multi-channel slotted ALOHA protocol where instead of uniformly spaced transmission slots in

This article has been accepted for publication in a future issue of this journal, but has not been fully edited. Content may change prior to final publication. Citation information: DOI 10.1109/TMC.2020.3000503, IEEE Transactions on Mobile Computing

multiple parallel subchannels, UORA uses TF-R triggered UL MU transmissions in multiple RA-RUs (see Fig. 1).[3]

Ever since the adoption of UORA, a number of 11ax meeting contributions recognized the above issue (low throughput). One workaround against low throughput (without any PHY modification) is to make the RA-RU transmissions as short as possible such that its effect on the system efficiency is minimal, while still benefiting from the multiple access gain [10], [11]. This is accomplished by transmitting a buffer status report poll (BSRP) trigger frame variant defined in the 802.11ax amendment. This is effectively a reservation ALOHA type scheme as has been seen in prior works even before the 802.11ax standardization (see [6] and [12]) whereby a small fraction of channel resources is initially spent on reservation for the subsequent (collision free) large payload transmission [13]. In the majority of use cases for UORA where the number of transmissions are high but the transmitted packets are very short (e.g. authentication and association frames, null data frames for power saving, etc.) [14], reservation ALOHA type of access is of little use (as there are no large payload to reserve RUs for).

In order to achieve random access with normalized throughput greater than 37%, it was shown in [7] that a form of subchannel level carrier sensing is required. Recognizing this, the authors proposed the MC-CSMA method which showed substantial improvements in normalized throughput compared to both slotted ALOHA and single channel CSMA. However unlike the trigger based approach of UL transmissions in 802.11ax, MC-CSMA is non-trigger based, i.e. STAs can transmit independent of any control/trigger by the AP. The difference between the non-trigger based and trigger based UL OFDMA can be seen in Fig. 2. Note that in Fig. 2(a), the fully distributed subchannel access results in some sparsity that can reduce the normalized throughput especially in non-saturated traffic conditions. In Fig. 2(b) on the other hand, this is not a problem as the AP can adjust the frequency of the TF schedule to match the offered load, allowing legacy BSS networks fair access to the channel. To the best of the authors knowledge, H-

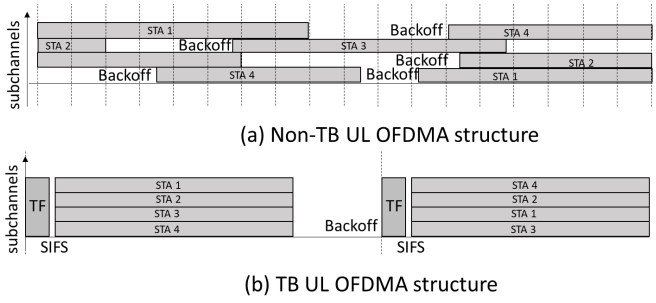

Fig. 2. Comparison of UL OFDMA PHY structures.

UORA is the first TB-MC-CSMA type access mechanism to be reported in literature. Based on the UL OFDMA PHY

3. Even with the higher total throughput (due to the increased bandwidth) compared to the single channel slotted ALOHA, the maximum *per-channel* throughput of multi-channel ALOHA is still 37%. The corresponding increase in the idle channel probability with multiple channels leaves the per-channel normalized throughput unchanged with respect to single-channel in theory, and in practice [9] a bit worse.

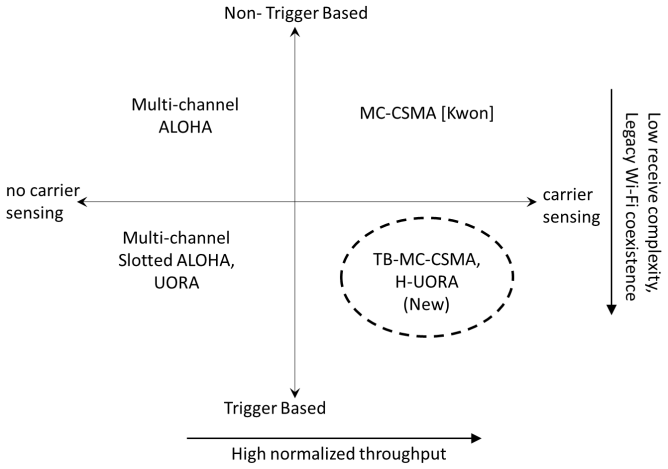

Fig. 3. Four types of multi-channel random access methods based on OFDMA.

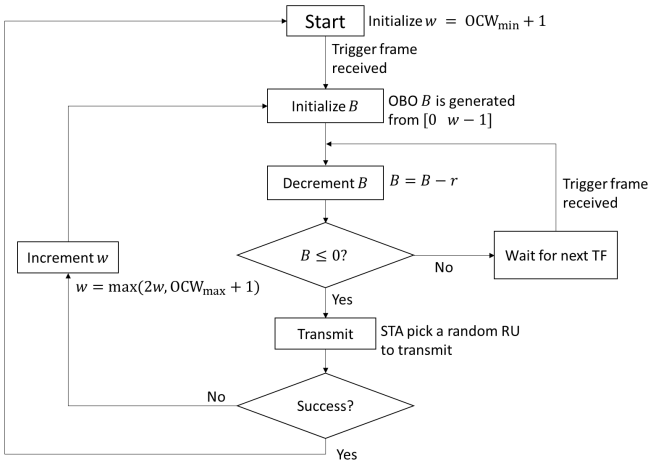

Fig. 4. 802.11ax UORA flowchart.

structures and presence of subchannel carrier sensing, we can categorize four types of multi-channel random access schemes as illustrated in Fig. 3. Schemes that do not require a TF are in the top half, while those that do are in the bottom half. Aside from the mentioned problems of non-trigger based methods, their implementations also present a design challenge as the receiver must always be ready to receive a new packet on one RU while it is receiving on another RU. Since packets in trigger based methods arrive at the same time, the receiver can process them as if it is a single effective packet, using a single Fast Fourier Transform (FFT) circuit [1].

3 802.11ax UORA Analysis

3.1 Access Protocol

A typical flowchart for the STA actions under the UORA mechanism is shown in Fig. 4. Every time a STA attempts a transmission, the STA generates an OBO count B uniformly chosen in the range of $[0, w-1]$ where w is the OFDMA contention window (OCW) size. During the first attempt, w

is set to the minimum contention window size $\mathrm{OCW}_{\min}+1$.[4] The STA then decrements the OBO by an amount equal to the number of RA-RUs r every time it receives a TF-R. When the OBO is reduced to less than or equal to 0, the STA is finally able to transmit, choosing an RA-RU randomly. When the STA fails to receive an acknowledgement, the STA assumes collision has occurred and hence would retry access. For every collision, w is updated to $2 \times w$ until w reaches the value of $\mathrm{OCW}_{\max}+1$. For notational simplicity, we refer to $\mathrm{OCW}_{min}+1$ as W, whereas W_i refers to the OCW sizes at the i^{th} retry, i.e.

$$W_i = \begin{cases} 2^i W & \text{if } 0 \leq i < m \\ 2^m W & \text{otherwise} \end{cases}. \tag{1}$$

Hence, succeeding retransmissions after m will use $\mathrm{OCW}_{\max}+1$ as the OCW size until the STA receives an acknowledgement. Note that m can be regarded as the maximum number of backoff stages and can be computed by

$$m = \log_2 \frac{\mathrm{OCW}_{\max}+1}{\mathrm{OCW}_{\min}+1}. \tag{2}$$

3.2 UORA Transmit and Collision Probability

Due to the use of binary exponential backoff, the transmit probability in UORA is a function of the number of STAs, the number of RA-RUs, and the contention window limits. As we have derived in [5], this transmit probability can be computed by using a bi-dimensional Markov chain similar to the analytical method used by Bianchi [15] under the steady state assumption where the transmit probability is independent of the state of any STA. When $r = 2^c$ where $c \in \mathbb{Z}_{\geq 0}$, the STA transmit probability τ (for any given TF) as a function of W and m can be expressed as

$$\tau(W,m) = \begin{cases} 1 & \text{if } W_m - 1 \leq r \\ \frac{2r}{A(1-p)} & \text{if } W - 1 \geq r \\ \frac{2r}{B(1-p)} & \text{if } W - 1 < r < W_m - 1 \end{cases} \tag{3}$$

where

$$A = W\frac{1-p-(2p)^m}{1-3p+2p^2} + \frac{r-2}{1-p} + \frac{2r}{W}\cdot\frac{2-p+p(\frac{p}{2})^m}{2-3p+p^2} \tag{4}$$

and

$$B = A + (r+2)\frac{1-p^{c+1}}{1-p} - \frac{1-(2p)^{c+1}}{1-2p}W + \frac{2r}{W}\cdot\frac{1-(p/2)^{c+1}}{1-p/2}. \tag{5}$$

Given the steady state transmit probability, the collision probability p experienced by a STA also becomes constant with respect to its state. Thus,

$$p = 1-(1-\frac{\tau}{r})^{n-1} \tag{6}$$

where n is the number of STAs. The equations (3-6) then form a system of nonlinear equations that can be solved to yield exact values of the transmit and collision probability for any values of W, m and r.

After solving for τ and p, one can obtain the probability P_s that an RA-RU is successful as

$$P_s(\tau) = n\frac{\tau}{r}(1-\frac{\tau}{r})^{n-1}. \tag{7}$$

Similarly, the probability P_i that an RA-RU is idle can be expressed as

$$P_i(\tau) = (1-\frac{\tau}{r})^n \tag{8}$$

while the probability P_c that an RA-RU is in collision as

$$P_c = 1 - P_s - P_i. \tag{9}$$

By taking the derivative of (7) with respect to τ and equating it to 0, the maximum successful RA-RU probability is achieved when

$$\hat{\tau} = \frac{r}{n}. \tag{10}$$

This results in equal successful and idle RA-RU probabilities of

$$P_s(\hat{\tau}) = P_i(\hat{\tau}) = \left(1-\frac{1}{n}\right)^n. \tag{11}$$

which asymptotes to $e^{-1} = 0.37$ for large n. Hence at best, conventional UORA suffers from a relatively large idle RA-RU probability of 0.37 and collision RA-RU probability of 0.26. In the next sections, we show how we break this limit by reducing the idle RA-RU probability without a corresponding increase in the collision probability (e.g. simply increasing the traffic reduces the idle RA-RU probability but also increases the collision RA-RU probability) resulting in a much higher successful RA-RU probability.

4 Trigger Based Multi-carrier CSMA

In this section, we first demonstrate the concept of TB-MC-CSMA using a simple example where STAs have exactly one chance to detect idle RUs using RU granulated carrier sensing before transmitting. Similar to DCF, RU sensing is done within a fixed duration - an RS slot. For illustration, Fig. 5(a) shows the conventional UORA scheme with 2 RA-RUs and 2 STAs. STA 1 generates an OBO count of 2 and because there are 2 RA-RUs, it is allowed to transmit on the succeeding UL OFDMA transmission opportunity. STA 1 randomly picks RA-RU 1 and transmits at time t_0. STA 2 on the other hand generated an OBO count of 3 which will be decremented down to 1 after the 2 RA-RUs. Under the rules of the conventional UORA, it needs to wait for another TF-R to resume its backoff.

4.1 $U = 1$ RS slot

In Fig. 5(b), STAs that have remaining OBO counts are allowed to continue to decrement their OBO as long as there are remaining idle RUs. The RU sensing is done at t_0 for a fixed duration of δ_{RS} which we refer as the RS slot duration. After sensing that RA-RU 2 is idle, STA 2 decrements its OBO from 1 to 0 which allows it to transmit at t_1. In the simple example above, RU sensing was able to almost double the throughput of UORA with the same allocated bandwidth.[5]

4. $\mathrm{OCW}_{\min}$ and $\mathrm{OCW}_{\max}$ are UORA parameters that are advertised by the AP using an information element in the Beacon and association response frames.

5. The increase is slightly less than double due to the δ_{RS} overhead.

This article has been accepted for publication in a future issue of this journal, but has not been fully edited. Content may change prior to final publication. Citation information: DOI 10.1109/TMC.2020.3000503, IEEE Transactions on Mobile Computing

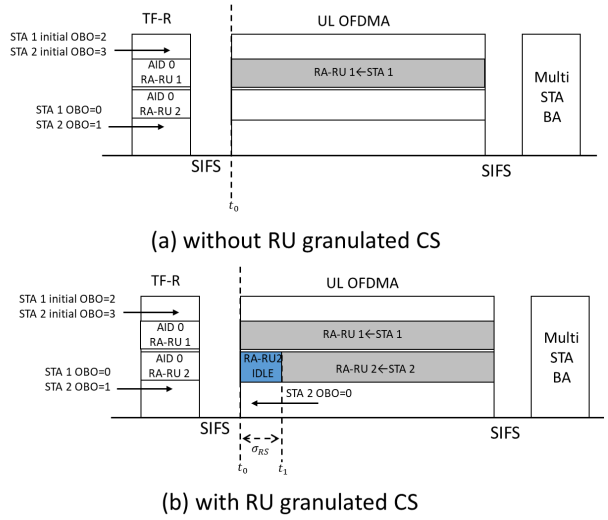

Fig. 5. UORA example with and without RU granulated carrier sensing.

In the general case with r RA-RUs and n STAs, the overall throughput will depend on the UORA access parameters (i.e. OCW_{min}, OCW_{max}). At time t_0, assume there are n_0 STAs contending for accessing the r_0 RA-RUs. At time t_1, n_0 reduces to n_1 (i.e. number of STAs that were idle after t_0) while r_0 reduces to r_1 (i.e. number of RA-RUs that were idle after t_0). For UORA with a single RS slot, let $P_{s,0}(1)$ and $P_{s,1}(1)$ be the probabilities that an RA-RU will be successful at time t_0 and t_1 respectively. The probability $P_s(1)$ that an RA-RU will be ultimately successful at the end of all time slots can then be expressed as

$$P_s(1) = \frac{r_0 P_{s,0}(1) + r_1 P_{s,1}(1)}{r_0} \tag{12}$$

$$= P_{s,0}(1) + \frac{r_1 P_{s,1}(1)}{r_0}. \tag{13}$$

It is clear from the above equation that maximizing $P_s(1)$ can be accomplished by maximizing $P_{s,0}(1)$ and $P_{s,1}(1)$ separately. First at time t_0, we know that there are n_0 STAs contending to access r_0 RA-RUs. From (7), the success probability can be expressed as

$$P_{s,0}(1) = n_0 \frac{\tau_0}{r_0} \left(1 - \frac{\tau_0}{r_0}\right)^{n_0 - 1} \tag{14}$$

where τ_0 refers to the transmit probability at t_0.

For transmissions during t_1, both r_1 and n_1 are random variables that depend on the number of STAs and idle RA-RUs after transmissions during t_0. Considering that the event of STA not transmitting during t_1 is a Bernoulli trial with a success probability of $(1 - \tau_0)$, n_1 can be modeled as a binomial random variable

$$p_{n_1}(k) = \binom{n_0}{k} (1 - \tau_0)^k \tau_0^{n_0 - k}. \tag{15}$$

It then follows that the expected number of contending STAs at t_1 can be expressed as

$$\bar{n}_1 = n_0 (1 - \tau_0). \tag{16}$$

Similarly, the event that an RA-RU will be idle after t_0 is a Bernoulli trial with a success probability of $\left(1 - \frac{\tau_0}{r_0}\right)^{n_0}$. The distribution of r_1 can thus be expressed as

$$p_{r_1}(k) = \binom{r_0}{k} \left[\left(1 - \frac{\tau_0}{r_0}\right)^{n_0}\right]^k \left[1 - \left(1 - \frac{\tau_0}{r_0}\right)^{n_0}\right]^{r_0 - k} \tag{17}$$

while its expected value can be expressed as

$$\bar{r}_1 = r_0 \left(1 - \frac{\tau_0}{r_0}\right)^{n_0}. \tag{18}$$

Due to the fact that the transmission during t_1 is a pure UORA (i.e. no further RU granulated carrier sensing is possible), the maximum value of $P_{s,1}(1)$ is e^{-1} for sufficiently large n_1 when the transmit probability is $\hat{\tau}_1 = \frac{r_1}{n_1}$. Hence from (13), we can write the maximum $P_s(1)$ as a function of τ_0,

$$\tilde{P}_s(1) = n \frac{\tau_0}{r_0} \left(1 - \frac{\tau_0}{r_0}\right)^{n_0 - 1} + e^{-1} \frac{r_1}{r_0}. \tag{19}$$

To further simplify the expression, we replace r_1 by its expected value expressed in (18) to get

$$\tilde{P}_s(1) \approx n_0 \frac{\tau_0}{r_0} \left(1 - \frac{\tau_0}{r_0}\right)^{n_0 - 1} + e^{-1} \left(1 - \frac{\tau_0}{r_0}\right)^{n_0}. \tag{20}$$

By taking the derivative $\frac{d\tilde{P}_s}{d\tau_0}$ and equating it to zero, we can obtain the transmission probability at t_0 that results in the maximum normalized throughput as

$$\hat{\tau}_0 = \frac{1 - e^{-1}}{n_0 - e^{-1}}. \tag{21}$$

Substituting this to (20), we get

$$\hat{P}_s(1) = \left(1 - \frac{1 - e^{-1}}{n_0 - e^{-1}}\right)^{n_0 - 1} \tag{22}$$

which represents the maximum success probability when both τ_0 and τ_1 are optimized. For $n_0 >> 1$, (21) and (22) approximates to

$$\hat{\tau}_0 \approx \frac{1 - e^{-1}}{n_0}, \tag{23}$$

$$\hat{P}_s(1) \approx e^{e^{-1} - 1} = 53\%. \tag{24}$$

which shows a notable increase of success probability compared to the maximum of 37% from the conventional UORA.

4.2 $U > 1$ RS slots

In general, the maximum RA-RU success probability for TB-MC-CSMA with U-RS slots can be obtained using the same methodology in (13) and applying mathematical induction. Assume that a $U-1$ RS slot TB-MC-CSMA has a maximum RA-RU success probability of $\hat{P}_s(U-1)$ obtained using a transmit probability of τ_0' at t_0, a U-RS slot TB-MC-CSMA can be realized using the following steps

1) Prepend an additional RS slot at the head of the $U-1$ RS slot TB-MC-CSMA as shown in Fig. 6.
2) Enforce the transmit probability of τ_0' at t_1
3) Recompute the optimal transmit probability at t_0 using

This article has been accepted for publication in a future issue of this journal, but has not been fully edited. Content may change prior to final publication. Citation information: DOI 10.1109/TMC.2020.3000503, IEEE Transactions on Mobile Computing

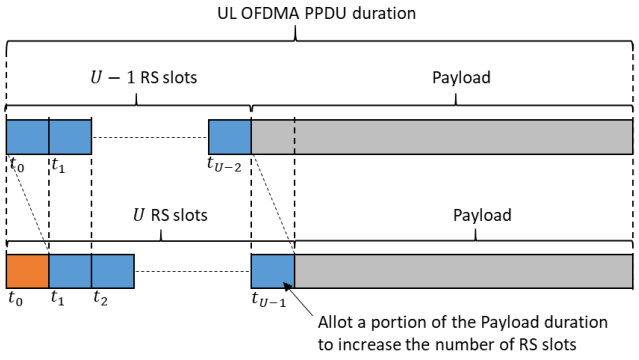

Fig. 6. RU sensing slot extension.

$$\tilde{P}_s(U) = n_0 \frac{\tau_0}{r_0}\left(1-\frac{\tau_0}{r_0}\right)^{n_0-1} + \hat{P}_s(U-1)(1-\frac{\tau_0}{r_0})^{n_0}. \tag{25}$$

It is easy to show that the maximum RA-RU success probability at t_0 for the U-RS slot TB-MC-CSMA is now achieved by

$$\hat{\tau}_0(U) = \frac{r_0}{n_0}[1-\hat{P}_s(U-1)]. \tag{26}$$

Substituting (26) to (25), the maximum RA-RU success probability is obtained as

$$\hat{P}_s(U) = e^{\hat{P}_s(U-1)-1}. \tag{27}$$

Considering that $\hat{P}_s(0) = e^{-1}$ (i.e. conventional UORA success probability), we can now compute the maximum RA-RU success probability for any value of U recursively using (27). The computed values of this maximum RA-RU success probability function is shown in Fig. 7. From (27), it is easy

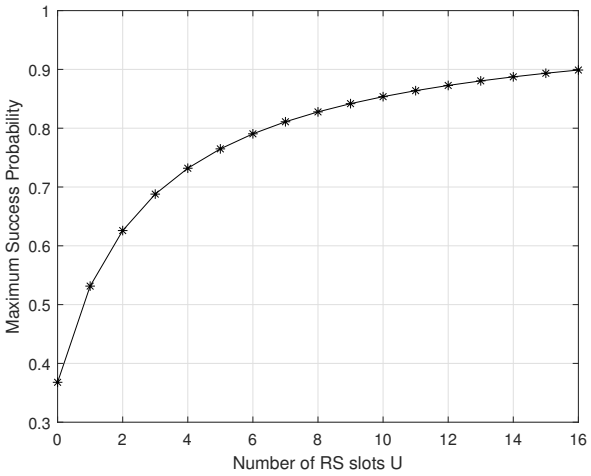

Fig. 7. Maximum success probability vs number of RS slots of TB-MC-CSMA.

to show that the maximum RA-RU success probability can be made arbitrarily close to 100% for sufficiently large U. However from Fig. 7, we see that beyond $U = 6$, the rate of increase does not warrant further increases in U. Hence we suggest a target success probability of 80%, achieved with $U = 7$ RS slots. In the remainder of this paper, we do not consider RS slots higher than $U = 7$ because of this.

Applying recursion to (26) and (27), we can express all the transmit probabilities for a U-RS slotted TB-MC-CSMA that maximizes the RA-RU success probability, as

$$\hat{\tau}_u = \begin{cases} \frac{r_U}{n_U} & \text{if } u = U \\ \frac{r_u}{n_u}[1-\hat{P}_s(U-u-1)] & \text{if } 0 \le u < U \end{cases} \tag{28}$$

where r_u and n_u represent the number of available RA-RUs and number of contending STAs at time slot u. Hence any practical implementation of TB-MC-CSMA need to ensure that these transmit probabilities occur at each of the $U+1$ transmit slots. In the proposed H-UORA algorithm, we approximate this requirement by replacing the random terms r_u and n_u in (28) by their expected values $\bar{r}_u$ and $\bar{n}_u$ respectively.

5 Proposed Algorithm: H-UORA

In a nutshell, the proposed H-UORA method is the standard UORA equipped with an added secondary backoff mechanism based on the TB-MC-CSMA. As seen in (28), making $\hat{\tau}_u$ a function of the time slot u provides more degrees of freedom compared to the conventional UORA backoff mechanism that is only controlled by OCW_{min}, OCW_{max}, and r which are not sufficient for tuning the $U+1$ time slot transmit probabilities of TB-MC-CSMA. In this section, we present how the proposed H-UORA is able to approximate the transmit probabilities (28) systematically.

1) Using the conventional UORA OBO mechanism (referred to in H-UORA as the primary backoff), STAs that has $\text{OBO} = 0$ after the current TF-R constitute a *transmitting set*.
2) STAs in the transmitting set use the TB-MC-CSMA to access the r RA-RUs along the $U+1$ transmit slots. STAs that cannot transmit before the RA-RUs deplete will be deemed to have had collided (i.e., increase the OCW and generate a new OBO).

Note that similar to UORA, any STA in the transmitting set of H-UORA will either be successful (in which case, the STA will reset its OCW) or result in collision (in which case, it doubles its OCW) after the TB-MC-CSMA phase. Because of this, the H-UORA primary backoff state follows the same UORA state machine albeit now with a lower collision probability than given by (6).

5.1 H-UORA PPDU format

The proposed H-UORA PPDU format that supports slotted TB-MC-CSMA is shown Fig. 8. Being based on the HE-TB PPDU, backward compatibility and coexistence with 802.11n/ac/ax PPDU formats are guaranteed. Note that the legacy short training field (L-STF) up to the high efficiency short training field (HE-STF) has the same functions as their 11ax PPDU counterpart (i.e. L-STF is for initial synchronization, while HE-STF is for MIMO gain control). These symbols also occupy the entire transmission bandwidth to serve as a backward compatibility and coexistence mechanism. After the HE-STF, STAs that transmit at the first time slot (i.e. at t_0) will proceed transmitting their HE-LTF and DATA

This article has been accepted for publication in a future issue of this journal, but has not been fully edited. Content may change prior to final publication. Citation information: DOI 10.1109/TMC.2020.3000503, IEEE Transactions on Mobile Computing

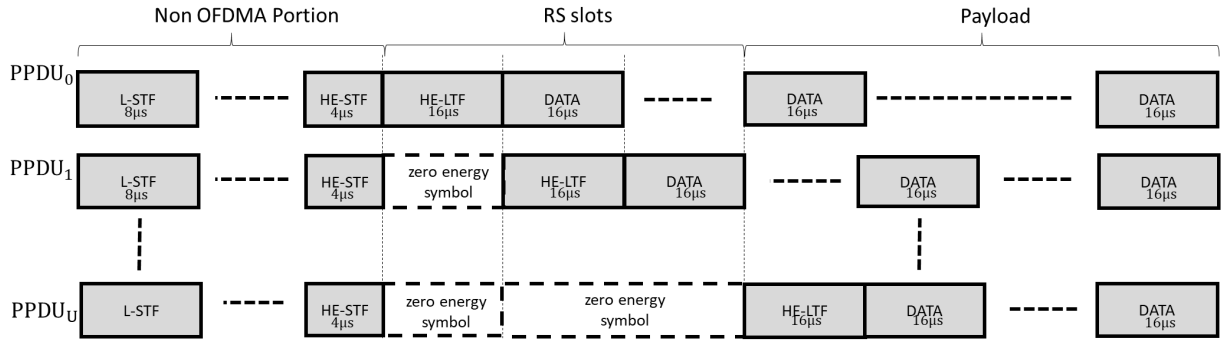

Fig. 8. PPDU format for H-UORA.

symbols as described by the 'PPDU$_0$' PPDU format. Since this is exactly the 11ax format for triggered UL MU PPDU, STAs that do not support RU granulated carrier sensing (e.g. 11ax STAs) can likewise participate in the transmission using this PPDU format.

Since the HE-LTF and DATA symbols of STAs transmitting at the previous time slot only occupy that RA-RU that they chose, the remaining STAs can perform RU sensing to detect which of the remaining RA-RUs are idle. Note that while performing RU sensing, STAs are in quiet duration mode corresponds to the zero energy OFDM symbols found in Fig. 8. When they finally transmit, they do so starting from their own HE-LTF followed by their DATA symbols. The transmitted PPDU will be one of the U PPDU formats in Fig. 8. At the AP, the received power at each RA-RUs are checked against a certain busy threshold to detect whether there is a transmission.[6] If an RA-RU is found busy at the start of some time slot t_i, the AP will buffer the received signal in the RA-RU until t_U. At this point, all signals from each RA-RUs would have already arrived and it can proceed to process them similar to conventional UORA. Note that RS slot duration is assumed to be 16µs corresponding to the maximum duration of an HE-LTF symbol. The accuracy and implications of this choice is discussed in Section 8.

5.2 OBO Based Primary Backoff

The H-UORA primary backoff determines the transmission set that will participate in every TB-MC-CSMA phase. At t_0, the total number of transmitting STAs and available RA-RUs can be expressed as

$$n_0 = n\tau(W, m), \tag{29}$$

$$r_0 = r \tag{30}$$

respectively. A portion of the transmitting set will transmit at t_0 while the rest will transmit at succeeding slots as determined by the H-UORA secondary backoff mechanism that will be discussed below. Note that since $\tau(W, m)$ is being adapted automatically by the binary exponential backoff during collisions, n_0 likewise will automatically adapt to optimize H-UORA without additional control from the user.

6. Using the TF, the AP sets the target received power at all RA-RUs. Hence, the busy power threshold can be set to some value below this target received power.

5.3 TB-MC-CSMA Based Secondary Backoff

For the H-UORA secondary backoff, we use the well studied p-persistent CSMA to determine at which slot a STA will transmit. Starting from the first slot $u = 0$, a STA generates a uniform random number $X_u \in (0, 1)$ to compare to a p-persistent CSMA transmit probability parameter ρ_u. If $X_u < \rho_u$, the STA transmits. Otherwise, it defers and performs RU sensing. If at least one idle RU exist, the STA will retry transmission on the next time slot $u = 1$.

Based on Section 3, the ideal value of ρ_u is $\hat{\tau}_u$ expressed in (28). However, its implementation is difficult due to the probabilistic nature of both r_u and n_u. We thus approximate these values by their expected values using (16) and (18) obtaining

$$r_u \approx \bar{r}_u = \begin{cases} r & \text{if } u = 0 \\ \bar{r}_{u-1}\left(1 - \frac{\rho_{u-1}}{\bar{r}_{u-1}}\right)^{\bar{n}_{u-1}} & \text{if } 0 < u \leq U \end{cases}, \tag{31}$$

$$n_u \approx \bar{n}_u = \begin{cases} n\tau\{W, m\} & \text{if } u = 0 \\ \bar{n}_{u-1}\left(1 - \rho_{u-1}\right) & \text{if } 0 < u \leq U \end{cases}. \tag{32}$$

Let

$$\kappa_u = \frac{\bar{r}_u}{\bar{n}_u}, \tag{33}$$

instead of (28), we set ρ_u as

$$\rho_u = \begin{cases} \kappa_u & \text{if } u = U \\ \kappa_u[1 - \hat{P}_s(U - u - 1)] & \text{if } 0 \leq u < U \end{cases}. \tag{34}$$

One problem with a p-persistent CSMA type backoff is that due to its probabilistic nature, STAs in the transmit set encounter long access delays when ρ_u is too low. Hence a desirable strategy - to guarantee that a STA transmits under H-UORA with U RA-RU slots - is to impose the boundary constraint $\rho_U = 1$, which from (34) translates to

$$\kappa_U = 1. \tag{35}$$

From (31) and (32), it follows that

$$\kappa_u = \kappa_{u-1}\frac{\left(1 - \frac{\rho_{u-1}}{\bar{r}_{u-1}}\right)^{\bar{n}_{u-1}}}{(1 - \rho_{u-1})} \tag{36}$$

$$= \kappa_{u-1}\frac{\left(1 - \frac{1-\hat{P}_s(U-u)}{\bar{n}_{u-1}}\right)^{\bar{n}_{u-1}}}{1 - \kappa_{u-1}[1 - \hat{P}_s(U - u)]}. \tag{37}$$

This article has been accepted for publication in a future issue of this journal, but has not been fully edited. Content may change prior to final publication. Citation information: DOI 10.1109/TMC.2020.3000503, IEEE Transactions on Mobile Computing

Approximating for large $\bar{n}_{u-1}$,

$$\kappa_u \approx \kappa_{u-1} \frac{e^{\hat{P}_s(U-u)-1}}{1-\kappa_{u-1}[1-\hat{P}_s(U-u)]} \quad (38)$$

and from (27), we have

$$\kappa_u \approx \kappa_{u-1} \frac{\hat{P}_s[U-u+1]}{1-\kappa_{u-1}[1-\hat{P}_s(U-u)]}. \quad (39)$$

Rearranging,

$$\kappa_{u-1} \approx \frac{\kappa_u}{\kappa_u[1-\hat{P}_s(U-u)]+\hat{P}_s(U-u+1)}. \quad (40)$$

Using (40) and (35), we can now compute all the corresponding values κ_u recursively. By substituting the computed κ_u values into (34), we find the proposed H-UORA secondary backoff transmit probabilities ρ_u.

Numerical κ_u and ρ_u values for $U = \{1, 3, 5, 7\}$ are plotted in Fig. 9. First note that for $U > 1$, κ_0 is almost a constant value of 0.84. For ρ_0 on the other hand, the value continues to decrease as U increases. This property of the H-UORA secondary backoff transmit probabilities in effect deprioritizes transmissions at earlier time slots compared to the latter time slots, ensuring that all U RS slots are optimally used.

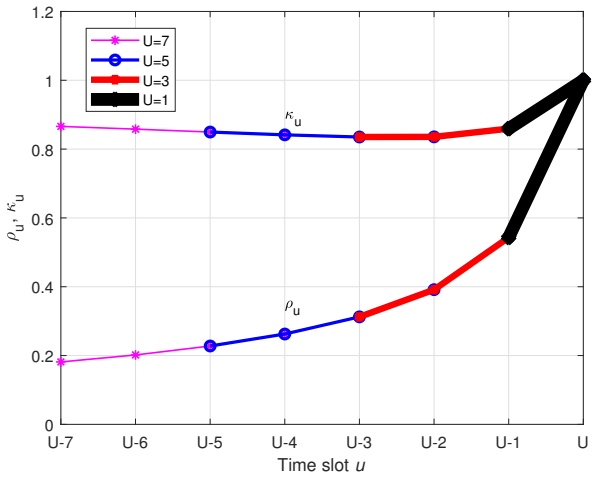

Fig. 9. H-UORA secondary backoff transmit probability ρ_u for $U = \{1, 3, 5, 7\}$.

5.4 Summary of H-UORA

The proposed H-UORA protocol is summarized in the Fig. 10 flowchart. Note that the upper portion is exactly the 802.11ax UORA backoff followed by the secondary backoff unique to the proposed H-UORA algorithm. After a STA gains TXOP from the primary backoff, it will perform a series of p-persistent CSMA trials using the probabilities ρ_u shown in Fig. 9 until it succeeds or no idle RUs remain. When at some time slot, no idle RUs remain, the STA will defer transmission and act as if it has experienced collision. It is important to note that the transmit probabilities plotted in Fig. 9 only depend on U, which is a local STA attribute.

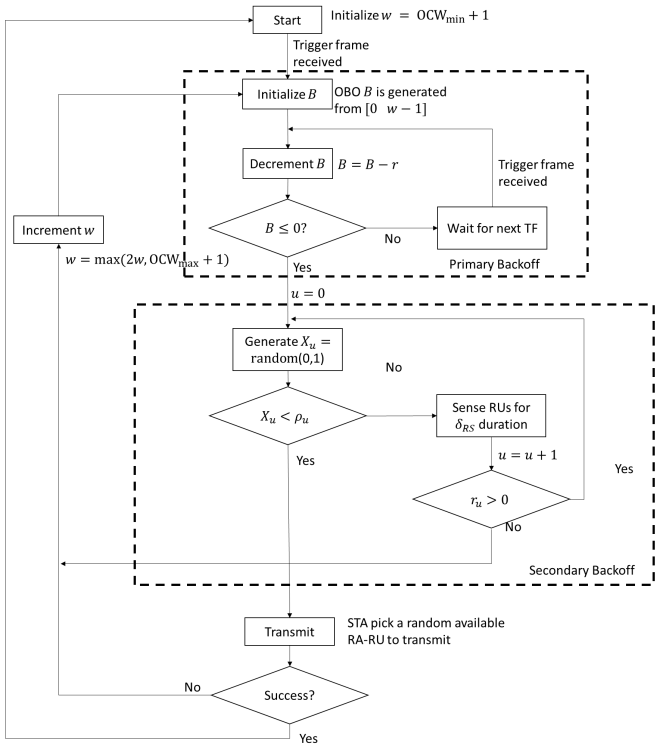

Fig. 10. Proposed H-UORA flowchart.

Hence no additional signaling is required for STAs to perform H-UORA apart from the already available $\text{OCW}_{\min}$ and $\text{OCW}_{\max}$.

To further illustrate H-UORA performance, observe Fig. 11 showing how four STAs (STA 1 - STA 4) that previously gained TXOP from the primary backoff process (i.e. STAs 1-4 are in the transmitting set) will perform the secondary backoff. First, the four STAs will transmit the non-OFDMA part of their preamble before starting the secondary backoff process. After the TF until just before t_0, all STAs would have generated their X_0 and compare them with ρ_0. In the figure, STA 3 succeeds so it proceeds to transmit its HE-LTF and payload at exactly t_0. From t_0 to t_1, STAs 1, 2 and 4 perform RU sensing and find that there are still 3 remaining RA-RUs, prompting them to perform another p-persistent CSMA trial- this time with respect to ρ_1. This time however, no STA succeeds, prompting all to repeat the RU sensing and p-persistent CSMA trial. Eventually, STA 1, STA 2 and STA 4 were able to transmit at t_2, t_3 and t_4 respectively. Note that STAs 1, 2 and 4 have a slightly shorter effective transmit duration compared to STA 3. Rate control algorithms must take this into account when deciding the transmission rate so as not to exceed the UL length set by the AP whenever the transmission occurs later inside the UL frame.

6 Numerical Results

In this section, we evaluate the performance of the proposed algorithm in terms of system throughput and latency. In order to isolate the performance gains due to the proposed H-UORA features, we assume that all STAs only use UORA or H-UORA for accessing the channel. For this, the AP

This article has been accepted for publication in a future issue of this journal, but has not been fully edited. Content may change prior to final publication. Citation information: DOI 10.1109/TMC.2020.3000503, IEEE Transactions on Mobile Computing

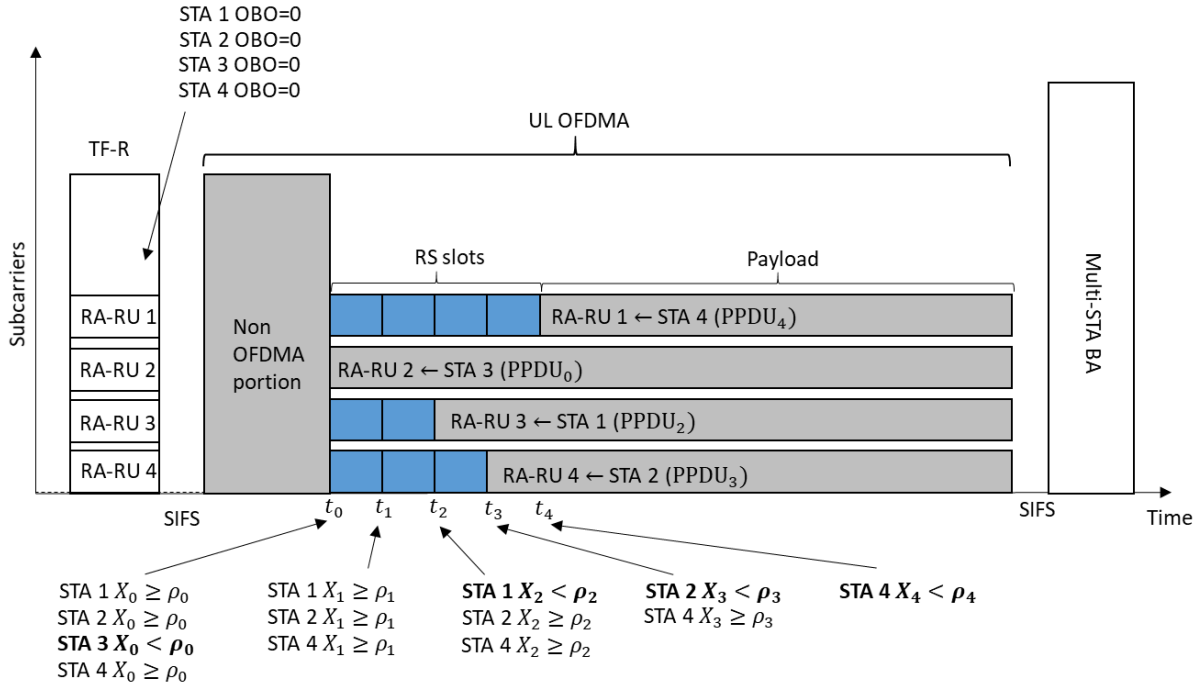

Fig. 11. Proposed H-UORA random access mechanism.

TABLE 2
Simulation Parameters

Parameter	Value
Packet Size	100/1500/10000 octets
RU size	26 tone
MCS	11 (PHY rate = 14.7Mbps/RU)
PHY preamble duration	56μs
Timeout duration	25μs
TF, TF-R duration	112μs
Multiuser BA duration	150μs
BSR duration	80μs
SIFS duration	16μs
PIFS duration	25μs
Offered Load	Full buffer

TABLE 3
Comparison of Analysis and Simulation Results: $r = 16$, OCW_{min}=15, OCW_{max}=127

n	Analysis P_s	Simulation P_s	Accuracy
5	0.217	0.216	99.4%
10	0.301	0.299	99.4%
20	0.359	0.357	99.6%
50	0.362	0.365	99.4%
100	0.287	0.286	99.9%

continuously sends a TF-R using the highest priority access (i.e. using a PIFS backoff instead of full duration exponential backoff) disabling any contention based access. Without any distributed contention based access, for STAs with full buffer offered load, evaluations can be reliably performed using a custom simulator in Matlab.[7] In all simulations, we used the default parameters listed in Table 2.

7. Simulation codes used in this paper are available in https://github.com/lanante/hybrid-uora

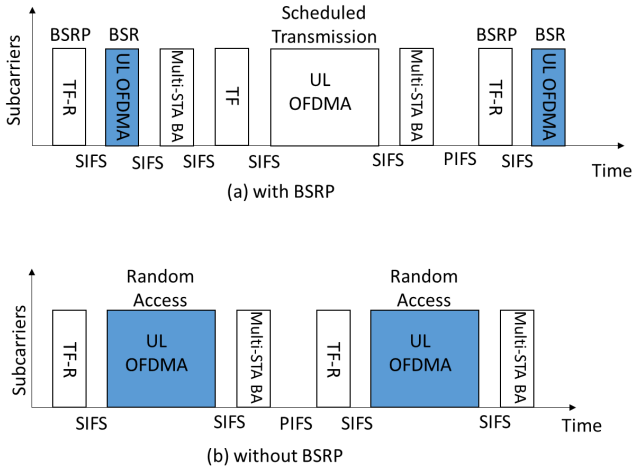

Fig. 12. UORA transmission sequences when successful.

First, we evaluate the accuracy of the Markov model analysis in Section 3 in predicting the performance of conventional UORA and the proposed H-UORA algorithms. For this study, we used $\text{OCW}_{min} = 15$ and $\text{OCW}_{max} = 127$ and ran the simulation to produce 20 seconds of data. The results for P_s are summarized in Table 3 having very high ($> 99\%$) agreement. Also notice that the maximum P_s is indeed about 0.37 as predicted by the analysis in Section 3.

Next, we evaluate the performance of H-UORA in terms of system throughput and latency. For comparison, we simulate the method proposed in [11] which uses the conventional UORA for BSR polling (henceforth, UORA-BSRP) followed by a scheduled transmission. Transmission sequences are shown in Fig. 12 in the case when the transmissions are

This article has been accepted for publication in a future issue of this journal, but has not been fully edited. Content may change prior to final publication. Citation information: DOI 10.1109/TMC.2020.3000503, IEEE Transactions on Mobile Computing

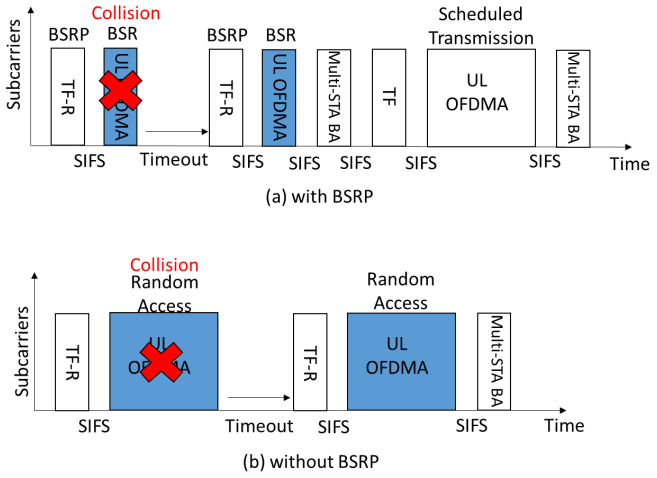

Fig. 13. UORA transmission sequences during collision.

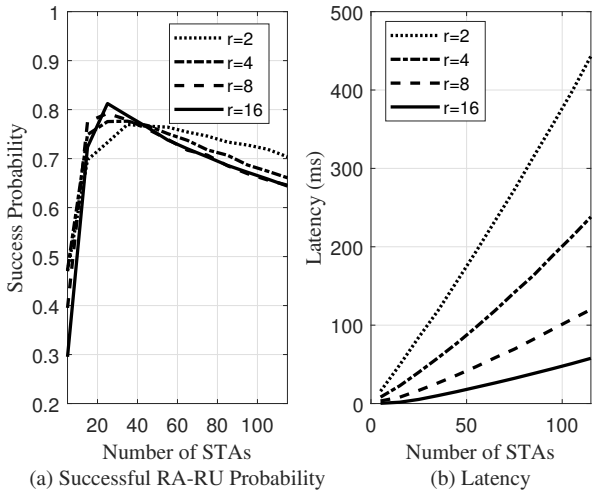

Fig. 16. H-UORA RA-RU success probability and latency: $U = 7$.

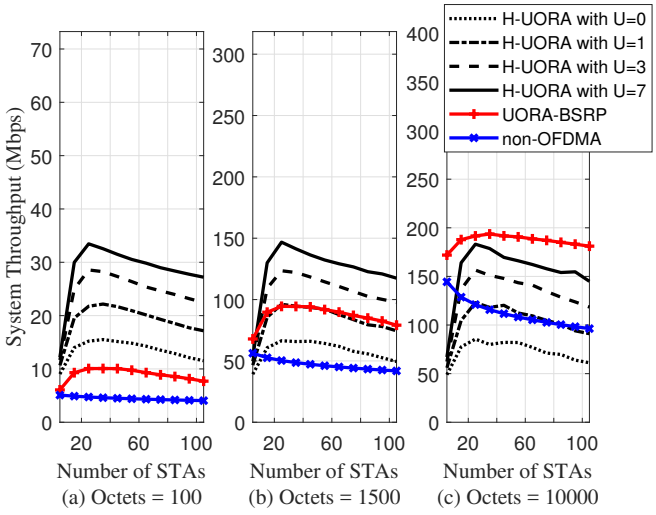

Fig. 14. H-UORA System throughput. r=16, OCW_{min}=15 and OCW_{max}=127 for H-UORA and UORA-BSRP; CW_{min}=15 CW_{max}=1023 for non-OFDMA.

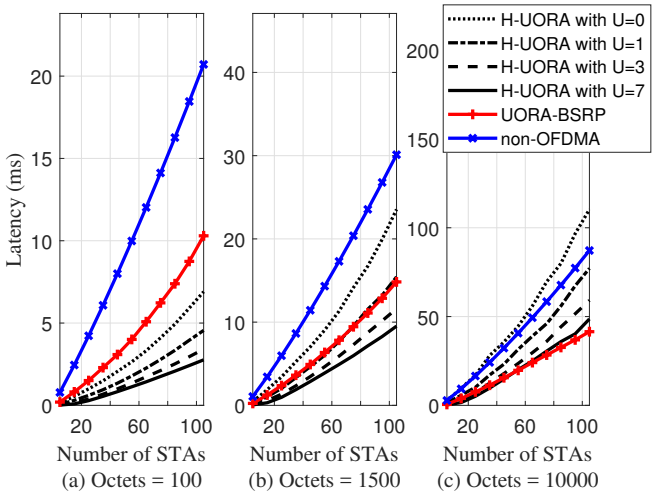

Fig. 15. H-UORA Latency. r=16, OCW_{min}=15 and OCW_{max}=127 for H-UORA and UORA-BSRP; CW_{min}=15 CW_{max}=1023 for non-OFDMA.

successful and Fig. 13 in the case when a collision occurs. Hence Figs 12(a) and 13(a) refer to UORA-BSRP while Figs 12(b) and 13(b) refer to H-UORA. For reference, we also plot the performance of a non-OFDMA system utilizing single carrier CSMA (see [16]) with a data rate of 235.2Mbps (i.e. equivalent to the data rate of all 16RUs at 14.7Mbps/RU). Note that since non-OFDMA STAs individually contend to use the whole channel bandwidth, their performance is relatively poor compared to both H-UORA and UORA-BSRP.

In Fig. 14(a), the system throughput as a function of the number of STAs is shown for short packet transmissions of 100 octets. We compare both the system throughput and latency at the reference number of STAs of 60 unless otherwise specified. Notice that for UORA-BSRP, the performance degrades by about 35% compared to the conventional UORA (i.e. H-UORA with $U = 0$ in the figure) due to the BSRP-BSR overhead. When the transmitted packet is increased to 1500 octets as in Fig. 14(b), the reduced collision penalty outweighs the BSRP-BSR exchange overhead resulting in a throughput gain of about 50%. As shown in Fig. 14(c), this gain increases further to 135% when all STAs transmit at 10000 octets.[8] For H-UORA on the other hand, Fig. 14 shows that it consistently achieved average throughput gains of about 40%, 80% and 110% (compared to conventional UORA) for $U = 1, 3$ and 7 respectively. These gains make H-UORA easily outperform both UORA-BSRP and non-OFDMA systems for both small and medium size packets. For very large packets, H-UORA with $U = 7$ lags by about 5-25% compared to UORA-BSRP indicating a possible need for $U > 7$ RS slots. Alternatively, as we will demonstrate in the next section, optimization of H-UORA primary backoff parameters can reduce this performance gap without the added hardware complexity involved with increased U. Finally, it is important to note that the system throughput degradation of UORA and H-UORA that occur when r is greater that the number of STAs can be mitigated

8. This is roughly the maximum number of octets that a STA can transmit in a 2MHz RU for MCS11 without exceeding the PPDU duration limit set by the standard.

This article has been accepted for publication in a future issue of this journal, but has not been fully edited. Content may change prior to final publication. Citation information: DOI 10.1109/TMC.2020.3000503, IEEE Transactions on Mobile Computing

by simply reducing r when the AP detects too many idle RA-RUs.

The latency of H-UORA - defined as the average duration a STA has to wait before successfully transmitting a packet via H-UORA - is shown in Fig. 15. In this paper, the latency is measured from the time the STA started H-UORA contention until the time the packet is correctly received by the AP.[9] Consistent with the system throughput results, H-UORA has the lowest latency in small and medium size packets and will be overtaken by UORA-BSRP as the packet size reach maximum. For H-UORA, the results suggest that 3 RS slots can reduce the latency by about 35% compared to conventional UORA. It is important to note that until now, the only way to effectively reduce the latency was to increase the number of RA-RUs which potentially decreases the per channel normalized throughput due to the increase in idle RUs. This downside is not present in H-UORA as the decrease of latency is now achieved due to the increased efficiency of using the available RA-RUs.

Next, in Fig. 16, we confirm that the success probability of H-UORA is very near the theoretical limit predicted in Fig. 7. For this simulation, we fixed the number of RS slots to $U = 7$ and vary the number of RA-RUs via $r = \{2, 4, 8, 16\}$. We observe a slight drop in maximum success probability from 0.81 to 0.76 when r is reduced to 2. Considering that our analysis assumed large values of n and r, this slight degradation shows the robustness of the proposed secondary backoff mechanism.

7 H-UORA Primary Backoff Optimization

TABLE 4
Optimal OCW_{min} and OCW_{max}; $U = 7$, $r = 16$

n	15	25	35	45	55	65	75	85	95
OCW_{min}	0	15	15	15	31	63	63	127	127
OCW_{max}	0	31	63	127	127	127	127	127	127

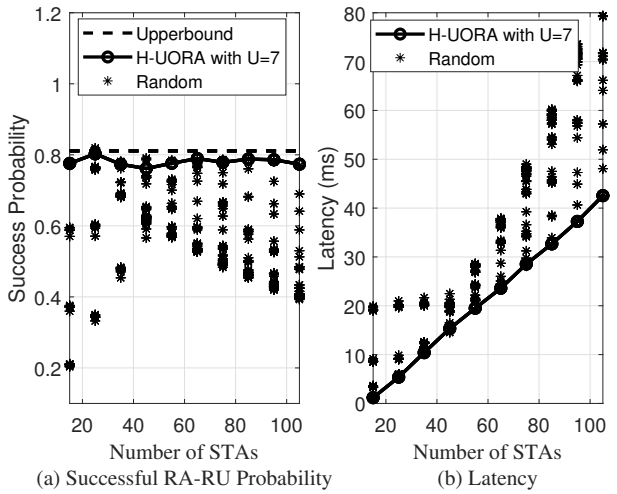

(a) Successful RA-RU Probability (b) Latency

Fig. 17. Optimized H-UORA performance: $U = 7$, $r = 16$.

9. This definition is analogous to the delay definition in [16].

Owing to the equivalence of the state machines describing H-UORA primary backoff and conventional UORA, access parameter optimization is very similar. For conventional UORA, it was shown in [5] that the optimal access parameters correspond to when the transmit probability $\tau(W, m)$ derived in (3) equals $\frac{r}{n}$ (the point where the success probability is 37%). Hence, finding the optimal access parameters can be done by

$$\tilde{W}, \tilde{m} = \arg\min_{W,m} \left| \tau(W, m) - \frac{r}{n} \right|. \tag{41}$$

In H-UORA, since the derived p-persistent CSMA probability ρ_u at each time slot is already optimal, what remains is to ensure that the transmit probability $\tau(W, m)$ will yield an optimal size of transmitting set vs. the number of RA-RUs. From (31) - (33), it follows that

$$\hat{\tau}(W, m) = \frac{r}{\kappa_0 n}. \tag{42}$$

It thus follows that the optimized parameters for H-UORA can be found by solving the problem

$$\tilde{W}\tilde{m} = \arg\min_{W,m} \left| \tau(W, m) - \frac{r}{\kappa_0 n} \right|. \tag{43}$$

Again, using the parameters in Table 2, we run the optimization problem in (43) using a full search algorithm with all possible values of OCW_{min} and OCW_{max}. The result is tabulated in Table 4 for $U = 7$ and $r = 16$.[10] The performance of these optimal values are then shown in Fig. 17 against random OCW_{min} and OCW_{max} values. As seen in Fig. 17(a), H-UORA is able to consistently perform near the upper bound of 0.81 for $U = 7$ regardless of n. The slight deviations can be explained by the fact that we can only approximately reach the optimal transmit probability $\frac{r}{n\kappa_0}$ as the allowed values of OCW_{min} and OCW_{max} are non-continuous. By optimizing the primary backoff parameters, the performance lag observed in Fig. 14(c), with very large packet sizes will stay at the minimum value of 5% regardless of n. The increased efficiency is also reflected in 17(b) where the proposed algorithm consistently produces the least latency regardless of n.

8 Other Considerations

8.1 RU sensing accuracy

All the results presented in this paper relies on the assumption that it is possible to sense the number of idle RA-RUs with perfect accuracy for the latency budget of 16µs. To shed light to the implications of this assumption, we consider a typical receive power spectrum shown in Fig. 19 for a 20MHz 802.11ax UL OFDMA transmission generated using the Matlab WLAN toolbox [17]. In the figure, each of the 9 RUs (26 tone) has a transmission coming from 9 STAs. A functional diagram of an RS circuit that detects the state of these RUs is shown in Fig. 18 (see [18] for a similar 20MHz carrier sense circuit). As shown, the circuit consists of digital bandpass filters, magnitude squaring, averaging and thresholding blocks. The magnitude square and averaging estimates the power of the signal located

10. As this can be done offline, the computational complexity of this step does not affect H-UORA real time performance.

This article has been accepted for publication in a future issue of this journal, but has not been fully edited. Content may change prior to final publication. Citation information: DOI 10.1109/TMC.2020.3000503, IEEE Transactions on Mobile Computing

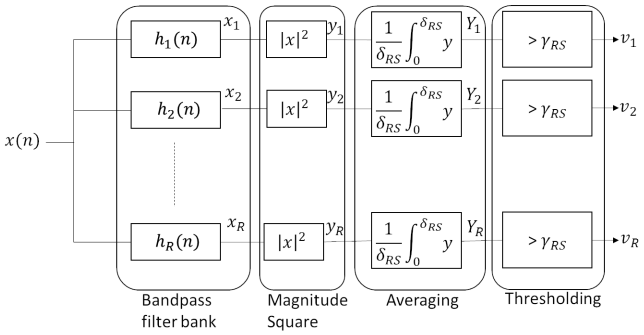

Fig. 18. RU granulated carrier sensing functional diagram.

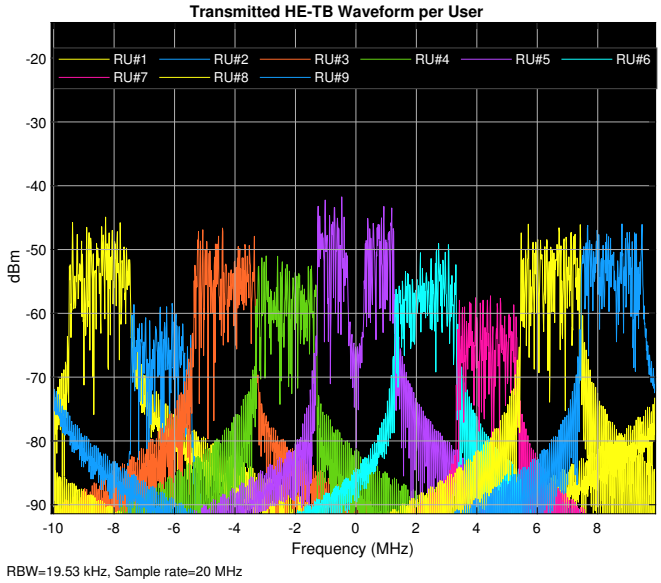

Fig. 19. Power spectrum of UORA signal.

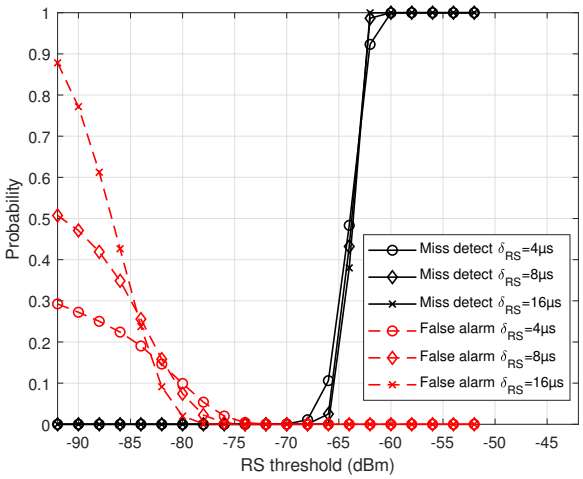

Fig. 20. RU sensing accuracy.

at each RU. We assume a filter bank consisting of 16-tap bandpass filters and a moving average block with window duration δ_{RS} of 4μs, 8μs and 16μs. As δ_{RS} is increased, the accuracy of the power estimation also increases at the expense of increased latency.[11] When this estimated power is greater than the set RS threshold γ_{RS}, the RU is declared busy.

Note that in Fig. 19, some RUs may have a lower power than others making it necessary to use a low γ_{RS}. When the γ_{RS} is too low, the power leakage due to the RU spectral sidelobe may cause false alarms. In Fig. 20, the probability of miss-detections and false alarms are shown. For the miss-detect probability, we simulated a UORA transmission where a -65dBm signal in a single 26 tone RU is received by a STA. For the false alarm probability on the other hand, we simulated a UORA transmission where a -65dBm signal in all but a single 26 tone RU are received by a STA. As seen in the figure, the RS circuit accurately detects the state of the RU as long as the threshold is less than the actual signal power by 1dB of margin for $\delta_{RS} > 8$μs. Moreover, setting the γ_{RS} to be greater than -82dBm (17dB below the adjacent RU power) makes the circuit robust to false alarms caused by power leakages. Hence in general, a STA using the example RS circuit in Fig. 18 can accurately perform RU sensing for an arriving signal when its power P_{rx} is between

$$\gamma_{RS} < P_{rx} < \gamma_{RS} + 17\text{dB}. \tag{44}$$

8.2 Hidden Node Problem

When miss-detections occur due to inaccurate RU sensing, a STA that accesses an RU using H-UORA may transmit on an already busy RU resulting in a collision. This is a type of hidden node problem that is unique to H-UORA.[12] A straightforward solution to this problem is by dynamic RS threshold control where the RS threshold is set based on the history of arriving signal power at each RU. When the RS threshold is set such that the incoming signal power satisfy (44), hidden nodes will not exist and H-UORA will perform as expected. Another approach for hidden node mitigation is for the AP to allocate non-adjacent RA-RUs such that power leakages from other RA-RUs can be ignored. Without power leakages, the STAs can set very low RS thresholds to eliminate any hidden nodes.

9 Conclusion

In this paper, we proposed a hybrid UORA scheme that uses carrier sensing to improve the normalized throughput of OFDMA based random access. Based on our analytical model, with enough RS slots, H-UORA can have a normalized throughput of near 100% in contrast to the 37% limit of conventional UORA. Due to the diminishing returns per additional RS slot however, we showed that H-UORA with 7 RS slots has a good balance between performance and complexity, achieving at least 80% of the total maximum throughput. The advantages of H-UORA against other access methods with higher normalized throughput include: 1. Unlike scheduled access, H-UORA does not require buffer status information from STAs, 2. Unlike MC-CSMA, H-UORA is interoperable with conventional UORA and finally

11. While all signal processing blocks contribute to the latency, most are small compared to the moving average block and hence ignored.

12. The well known legacy hidden node problem that occurs in contiguous 20MHz bandwidths and above are easily solved by using a Multi-RTS-CTS exchange prior to the UL OFDMA and hence not considered in this paper.

3. Unlike, UORA with BSRP, H-UORA maintains its high throughput even with small packets from STAs. The only disadvantage of H-UORA is that it requires a much finer carrier sensing circuit than what is required in the current 802.11ax amendment. But with increasingly heterogeneous nature of the license free bands, we expect that finer carrier sensing will be a necessary feature in the next iteration of 802.11ax WLANs.

REFERENCES

[1] *Draft Standard for Information Technology - Telecommunications and Information Exchange Between Systems - Part 11: Wireless LAN Medium Access Control (MAC) and Physical Layer (PHY) specifications - Amendment 6: Enhancements for High Efficiency WLAN, D6.0*, Draft IEEE Std. P802.11, 2019.

[2] B. Bellalta, "IEEE 802.11ax: High-efficiency WLANS," *IEEE Wireless Communications*, vol. 23, no. 1, pp. 38–46, February 2016.

[3] E. Khorov, A. Kiryanov, A. Lyakhov, and G. Bianchi, "A Tutorial on IEEE 802.11ax High Efficiency WLANs," *IEEE Communications Surveys Tutorials*, vol. 21, no. 1, pp. 197–216, September 2019.

[4] D. Bankov, A. Didenko, E. Khorov, and A. Lyakhov, "OFDMA Uplink Scheduling in IEEE 802.11ax Networks," in *IEEE International Conference on Communications*, May 2018, pp. 1–6.

[5] L. Lanante, T. Uwai, H. Ochi, Y. Nagao, M. Kurosaki, and C. Ghosh, "Performance analysis of the 802.11ax UL OFDMA random access protocol in dense networks," in *IEEE International Conference on Communications*, May 2017, pp. 1–6.

[6] Y. P. Fallah, S. Khan, P. Nasiopoulos, and H. Alnuweiri, "Hybrid OFDMA/CSMA Based Medium Access Control for Next-Generation Wireless LANs," in *IEEE International Conference on Communications*, May 2008, pp. 2762–2768.

[7] H. Kwon, H. Seo, S. Kim, and B. G. Lee, "Generalized CSMA/CA Protocol for OFDMA Systems," in *IEEE Global Telecommunications Conference*, November 2008, pp. 1–6.

[8] C. Ghosh. Random Access with Trigger Frames using OFDMA. [Online]. Available: https://mentor.ieee.org/802.11/dcn/15/11-15-0875-01-00ax-random-access-with-trigger-frames-using-ofdma.pptx

[9] D. Shen and V. O. K. Li, "Stabilized multi-channel ALOHA for wireless OFDM networks," in *IEEE Global Telecommunications Conference*, vol. 1, November 2002, pp. 701–705 vol.1.

[10] W. Ahn, Y. Kim, and R. Kim, "An Energy Efficient Multiuser Uplink Transmission Scheme in the Next Generation WLAN for Internet of Things," *International Journal of Distributed Sensor Networks*, vol. 12, pp. 1 512 054–1 512 054, July 2016.

[11] R. Y. Kim, "Sub-channel Based Uplink OFDMA Random Access Scheme Considering Hidden Nodes in the Next Generation Wireless," *IOSR Journal of Engineering*, vol. 6, no. 1, 2016.

[12] G. Haile and J. Lim, "C-OFDMA: Improved Throughput for Next Generation WLAN Systems Based on OFDMA and CSMA/CA," in *International Conference on Intelligent Systems, Modelling and Simulation*, January 2013, pp. 497–502.

[13] W. Crowther, R. Rettberg, D. Walden, S. Ornstein, and E. Heart, "A system for broadcast communication: reservation-ALOHA," in *International Conference on Systems Sciences*, January 1973.

[14] J. Lansford. IEEE 802.11ax High Efficiency WLAN Packet measurements around Boulder, CO. [Online]. Available: https://mentor.ieee.org/802.11/dcn/14/11-14-0546-01-00ax-packet-traffic-measurements-around-boulder-colorado.ppt

[15] G. Bianchi, "Performance analysis of the IEEE 802.11 distributed coordination function," *IEEE Journal on Selected Areas in Communications*, vol. 18, no. 3, pp. 535–547, March 2000.

[16] G. Bianchi and I. Tinnirello, "Remarks on IEEE 802.11 DCF performance analysis," *IEEE Communications Letters*, vol. 9, no. 8, pp. 765–767, 2005.

[17] MATLAB v9.5 and WLAN System Toolbox v2.0. [Online]. Available: https://www.mathworks.com/help/wlan

[18] Y. Kim. CCA Using GI. [Online]. Available: https://mentor.ieee.org/802.11/dcn/10/11-10-0012-00-00ac-cca-using-gi.ppt

Leonardo Lanante Jr received the B.S. in Electronics and Communications Engineering degree and M.S. in Electrical Engineering from University of the Philippines, and Ph.D in Information Systems from Kyushu Inst. of Technology in 2005, 2007, and 2011 respectively. He is currently with the Kyushu Institute of Technology as an assistant professor in Computer Science and Systems Engineering department since 2014. His research interests include next generation WLAN technology including multiple access, MIMO-OFDM, and localization.

Chitabratta Ghosh did his postdoctoral research in the Electrical Engineering Department, University of Washington, Seattle, WA, USA. He is currently with the Intel Corporation, Santa Clara, CA, USA, and an Affiliate Assistant Professor with the University of Washington. He is an active contributor to IEEE 802.11ah, which is a long-range low-power amendment to the IEEE 802.11 wireless local area network standard, and was a member of the Executive Review Committee toward its draft development. His research interests include developing spectrum-sharing concepts for next-generation commercial communications systems and solving coexistence challenges among cooperating heterogeneous wireless networks. He is the author of more than 30 conference and journal publications and of over 30 filed or published patents. He has received the IEEE PACRIM Gold Award for Best Communications Paper in 2011 and the Best Paper Award at the IEEE PIMRC 2012. He is serving as an Editor for the IEEE TRANSACTIONS ON WIRELESS COMMUNICATIONS and is currently the Vice Chair of the IEEE Technical Committee on Simulations(TCSIM).

Sumit Roy (F07) received the B.Tech. degree from IIT Kanpur, Kanpur,and the M.S. and Ph.D. degrees from the University of California at Santa Barbara, all in electrical engineering in 1983, 1985, and 1988,respectively, and the M.A. degree in statistics and applied probability in 1988. He is currently an Integrated Systems Professor of Electrical Engineering, University of Washington. His research interests include analysis/design of wireless communication and sensor network systems with a diverse emphasis, emerging beyond 4G standards, multi-standard wireless internetworking and spectrum coexistence using cognitive radio platforms, terrestrial vehicular, aerial and underwater networks, and sensor and smart grid networking. From2001 to 2003, he was with the Intel Wireless Technology Lab as a Senior Researcher, where he was involved in systems architecture and standards development for ultra-wideband systems (wireless PANs) and next generation high-speed wireless LANs. He served as the IEEE ComSoc Distinguished Lecturer from 2014 to 2015.